Advanced Journal of Chemistry-Section A, 2020, *3*, S594–S611 (*Special Issue*)
Available online at : www.ajchem-a.com
ISSN Online: 2645-5676
DOI: 10.33945/SAMI/AJCA.2020.5.5

Original Research Article

Synthesis of Cross-Linked Carboxymethyl Legume Starch for Adsorption of Selected Heavy Metals from Aqueous Solutions

Ayodele Akinterinwa[a,*], Ebun Oladele[b], Albert Adebayo[b], Olubode Ajayi[b]

[a] *Department of Chemistry, Modibbo Adama University of Technology, Yola, Nigeria*
[b] *Department of Chemistry, Federal University of Technology, Akure, Nigeria*

ARTICLE INFO

Received: 27 December 2019
Revised: 29 February 2020
Accepted: 01 April 2020
Available online: 07 April 2020

KEYWORDS

Adsorption/sorption
Carboxymethylation
Cross-linking
Heavy metals
Legume starch

ABSTRACT

In this work, legume starch from Kwakil beans (*Phaseolus vulgaris* L.) was cross-linked with epichlorohydrin and carboxymethylated with different concentrations of sodium monochloroacetate (SMCA) (5-30% w/w of starch db). Degree of substitution (DS) of carboxymethyl group ranged between 0.02-0.063, and adsorption was enhanced as the DS increased. The native starch (NS), cross-linked starch (ECS), and the carboxymethyl derivative (ECCS-15%; DS=0.062) with optimum adsorption capacity in Pb^{2+} (98.51%) and Cd^{2+} (97.32%) aqueous solution were further characterized using FTIR and SEM-EDX. Equilibrium studies revealed that the adsorption of Pb^{2+} and Cd^{2+} from aqueous solution by ECCS increased by enhancing the pH, contact time (up to equilibrium time at 15 min), initial concentration and adsorbent dosage, but decreased with increasing the temperature and interfering ion (Na^{+} and Ca^{2+}) concentrations. Pb^{2+} data fits pseudo-second order kinetic (R^2=0.9999) and Langmuir isotherm models (R^2=0.9983), and ΔH=-48.67 Kj/mol^{-1}. This signals a chemisorption process. Pb^{2+} and Cd^{2+} can be recovered efficiently (up to 99%), and the adsorbent can be reused up to 5 cycles with sorption capacity above 75%. On application, ECCS reveals good potentials in the purification of wastewater with low heavy metal ion concentrations.

GRAPHICAL ABSTRACT

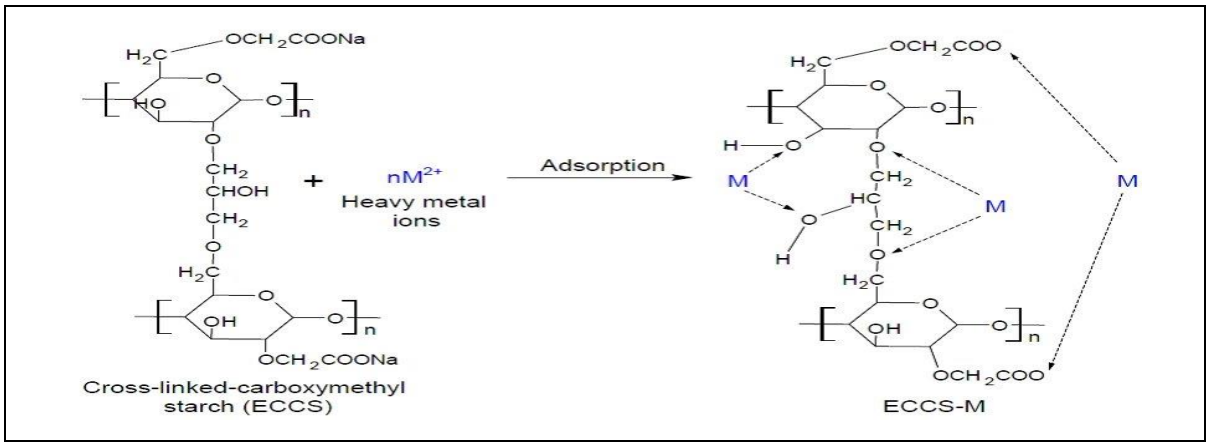

* Corresponding author's E-mail address: ayoterinwa@yahoo.com

Introduction

Regulating bodies may have to push towards zero tolerance of some heavy metals such as lead and cadmium in drinking water as reports of detrimental health effects of the present permissible levels are now emerging [1]. Lead and cadmium are potent neurotoxins, and the major sources are untreated and inadequately treated wastewaters from some mining and industrial processes due to the cost and efficiency of the wastewater treatment. This situation therefore calls for development of cheap and efficient treatment technologies, such that can be achieved from the aim of this study.

Starch is a natural raw material, abundant, renewable, and absolutely biodegradable. It is a biopolymer and the basic (monomer) units are glucose linked by linear α-(1→4), branched α-(1→6) with acetals at the linkages. Properties of starch may vary based on their botanical sources, modifications, and the materials/conditions of the modification process. Interactive hydroxyl groups and the oxygen atoms at the linkages (acetals) are the major functional groups on starch molecules, and these functional groups has been identified as potential adsorptive sites for metal ions [2,3]. However, the versatile modifications amenable to starch allows the introduction of other functional groups such as, esters, carbonyl, carboxylate, xanthate, phosphate/phosphoryl, carbamate, and acrylate, with affinity for some inorganic and organic water contaminants, *via* molecular, electrostatic and coordinative interactions resulting in the removal of the contaminants from water [4,5]. Cross-linking reaction is the introduction of inter-and intra-molecular bonds which results in a three-dimensional network in the starch polymer matrix. It impacts morphological reinforcement and mechanical stability of the starch polymer matrix, hence the granules [6]. The three-dimensional network in cross-linked starch has also create pores which may serves as trapping sites for contaminants in a phenomenon referred to as ultrafiltration [7]. Epichlorohydrin (C_3H_5ClO) is one of the starch cross-linking agents. Its reaction with starch is a multifunctional reaction that occurs over series of steps in which one or two molecules are consumed to form a single cross-link [8].

Swelling and water absorption are important properties of adsorbents, however, cross-linking may decrease this properties by increasing molecular compactness in starch granule [9]. To ameliorate these properties and improve the adsorption potentials of the cross-linked starch derivatives, further functionalization process such as carboxymethylation is necessary. Carboxymethylation introduce a hydrophilic carboxymethyl group ($-CH_2COO^+$) to starch derivatives, and this is achieved in the reaction with carboxymethyl derivative such as sodium monochloroaceteate [10]. Carboxymethyl group is constituted by carbonyl (C=O) and carboxylate ($-COO^+$) functional groups, and these have been associated with heavy metal adsorption *via* coordination, molecular bonding and ion-exchange processes [11-13].

Starch based adsorbents are porous functionalized materials with large surface area. They have been reported with some outstanding features including, renewability, rapid adsorption, easy and efficient pollutant recovery and adsorbent regeneration [14,15]. Starches from different botanical sources which can be categorized as *A*- and *B*-types have been extensively studied for the adsorption of heavy metal ions from aqueous solutions [14]. C-Type starches are with unique structural properties intermingling those of A- and B-Types [16, 17]. These have not been found in the archive of starch adsorbent studies. Legumes starches are categorized as C-Type starches. Some legumes are increasingly under-utilized as they fall out of the staple consumption due to their

poisoining tendencies. Clinical complications from the consumption of some variety of red kidney beans were reported by Kumar *et al.* [18]. In the report, toxicity associated with some typical components of the bean such as, lectins, saponins, phytates, and protease inhibitors, and allergenicity that induced by its allergenic proteins.

The objectives of this work are to synthesize and access the adsorption potentials of the cross-linked carboxymethyl legume starch. Starch extracted from Kwakil beans, a local variety of red kidney beans (*Phaseolus vulgaris*) was selected for this study. To investigate the success of the synthesis and application, chemical functionality, surface morphology, and elemental composition of the products were assessed using the FTIR, SEM and EDX, before and after they were used in the adsorption of lead and cadmium.

Experimental

Materials

Beans were obtained from local farmers in Mangu, Plateau State, Nigeria. The chemicals were supplied from Sigma–Aldrich Chemicals (St. Louis, MO, USA) and Merck (Darmstadt, Germany). Waltman filter paper No. 41 and fine mesh muslin cloths were obtained from the local chemical stores. All the chemicals were of analytical/synthesis grade. Wastewater samples were obtained from a crude oil exploration site (untreated produced water), Forcardos terminal, Ogulagha, Burutu Local Government, Delta State and a gold processing site in Nassarawa-Kanji, Kashegu Local Government, Niger State, Nigeria.

Extraction and evaluation of starch

Starch was extracted using method C reported by Schoch and Maywald [19], with slight modifications as follows; 1 Kg was soaked overnight in 4 L of 0.5% NaOH solution, after which the coats were removed. The cleaned beans were wet milled in a blender operated at low speed with ice cold 1% NaOH solution. The slurry was filtered through a fine mesh muslin cloth (300 μm maximum pore sizes), into a clean bowl of 5 L distilled water. A suspension was obtained, this was filter through doubled fine mesh muslin cloths, and the pH was adjusted to 8.0 with 0.1 M NaOH solution. The suspension was allowed to settle until a clear separation was observed (about 5 h). The supernatant was separated, and the slurry was re-dispersed and washed with distilled water three times before filtration using Whatman No 41 filter papers, drying in oven overnight at 40 °C, and grounding in a mortar. Starch yield was calculated from the mass of starch obtained as a percentage of the mass of beans soaked. Proximate analysis was carried out according to the AOAC [20]. Amylose content was determined while starch sample (1 mg) was shaken in a 6 mM iodine solution made by 90% DMSO and 10% water, till a complete dissolution was obtained (in about 7 h). The resultant solution was diluted further with 8 part deionized water, and left for 30 min for the iodine-amylose complex to form a stable colour, the absorbance of the solution and that of amylose standards were read at 620 nm against the reagent blank using UV spectrometer [21]. Three replicate experiments were carried out for each analysis.

Crosslinking and carboxymethylation of starch

Method by Kim and Lim [11], with modification in the carboxymethylation reaction according to Stojanovic *et al.* [22] was adopted. Starch (100 g, db) was dispersed in distilled water (300 mL) and EPI (1 mL of 99.9 assay reagent) from a micro-pipette was added. The pH of the mixture was adjusted to 11 (and the pH meter remain in contact), and the mixture was transferred to water bath equipped with stirrer. The reaction was

allowed for 3 h with continuous starring at 35 °C, while the pH was maintained at 11.0±0.2 with drops of 3% NaOH solution. Afterwards, the slurry was filtered with Whatman No. 41 filter paper, washed three times in 400 mL distilled water and set in the oven to dry at 40 °C to obtain ECS. In another round of the reaction, ECS after filtration was dispersed in 300 mL ethanol absolute, sealed and set to stir in the water bath at 50 °C. NaOH (40 mL of 40% solution) was added in drops (for about 15 min) before adding SMCA (5, 10, 15, 20 and 30% w/w, based on starch db), while NaOH was continuously added over 1 h. Stirring continue in the sealed container and the reaction was allowed for 2 h, after which the slurry was filtered, washed three times in 400 mL distilled water, adjusted to pH 8.0, and dried in the oven at 40 °C, to obtain ECCS.

Determination of degree of substitution (DS)

Degree of substitution was determined for ECCS derivatives by back titration method Stojanovic *et al.* [22]. ECCS derivatives (3 g, db) were dispersed in 20 mL of deionized water; HCl (3%) was added to the slurry to reduce the pH to 2.0, and stirred for 10 min to convert the carboxymethyl group to its hydrogen/free acid derivative. The starch was filtered and washed three times, and gelatinized in 40 mL deionized water by boiling (in water bath) for 30 min. The gelatinized free acid derivative was titrated with standardized 0.1 M NaOH solution, while ECS was used as a blank. The experiment was repeated three times for each derivative, and the mean titer value was used in calculating n_{COOH}, which was further used in calculating the DS as shown in Equation 1. Where M_{ds} is the mass of starch db and n_{COOH} is the number of moles of the free acid derivatives.

$$DS = \frac{n_{COOH} \times 162\ g.mol^{-1}}{M_{ds} - n_{COOH} \times 58\ g.mol^{-1}} \quad (1)$$

Characterization

Perkin Elmer FTIR spectrophotometer (England, UK) was used for the FTIR analysis. Samples were scanned (10 times) through KBr pellets within the wavelength range 4000-500 cm^{-1}. Scanning electron microscope (SEM) and energy dispersive X-ray (EDS) analysis was carried using the Bruker Nano GmbH Berlin, Germany with Esprit 2.0 software, fitted field emission source and operating at the accelerating voltage of 15 kV. Heavy metal ion concentrations were determined using the atomic adsorption spectrometer (AAS) (Buck Scientific 210 VGP). Pb^{2+} and Cd^{2+} were scanned at 217.0 and 228.8 nm wavelengths, with detection limit 0.06 and 0.02 ppm, respectively. Flame emission spectrometer (FES) (Jenway PFP7) was used to determine the Na^{+} concentration with detection limit of 0.10 ppm.

Sorption experiments

Pb^{2+} and Cd^{2+} stock solutions (1000 ppm) were prepared in double distilled water from pure grades of ($Pb(NO_3)_2$) and ($Cd(NO_3)_2$), and this was diluted to other concentrations used in the adsorption experiments. Adsorption experiments were carried out by 1% w/v of the adsorbents in aqueous solutions at 100 rpm on an obital shaker (CelTech KJ -201BD), at designated pH, time and temperature. Adsorption was determined from initial and final concentrations of ion in the filtrate solution as analysed using AAS and FES (for Na^{+}). Each sorption experiment was carried out twice (reproductivity is ± 3%), and the mean value was used in calculating percentage sorption (Equation 2) and sorption amount (Q) in mg/g (Equation 3).

$$\%\ sorption = \frac{C_0 - C_e}{C_0} \times 100 \quad (2)$$

$$Q\ (mg.g^{-1}) = \frac{(C_0 - C_e)\,V}{1000\,W} \quad (3)$$

Where C_0 is the initial concentration, C_e is the equilibrium/final concentration, V is the volume of aqueous solution in cm^3, and W is the weight of sorbent in gram.

Effect of pH on sorption was determined by shaking sorbent (1% w/v) in aqueous solutions within pH range 2 - 8, for 120 min at 30 °C. The solution pH was adjusted with 0.1 M solutions of NaOH and HCl. Sorption rate and the effect of time was studied within 2-240 min at 30 °C and optimum pH, and the kinetics studies were carried out by analyzing the sorption using the pseudo first order, pseudo second order, pseudo third order, Elovich, external diffusion and intra-particle diffusion models. Effect of the initial ion concentrations was studied within 10-200 ppm, at 30 °C, and optimum pH and time. Sorption isotherms were studied by evaluating the sorption data using the Langmuir, Freundlich, Temkin, Hesley and Dubinin-Radushkevich (RD) isotherm models. Effect of temperature was studied with 30-70 °C, at optimum pH and time. Thermodynamics studies were carried out by analyzing the data using the Van't Hoff's and thermodynamic equations. Effect of the sorption dose was studied by varying the dose from 0.5-3% (w/v), while ionic interference was studied using different concentrations (5-50 ppm) of NaCl and $CaCl_2$ at the optimum pH and time.

Desorption/regeneration and reusability studies

This was carried with slight modifications to the method by Kim and Lim [11]. ECCSs (1 g) used in the sorption of Pb and Cd were dispersed in 40 mL deionized water in two different beakers, and adjusted to pH 2.0 using 1 M HNO_3 solution. The slurries were separately stirred for 5, 10 and 15 min, filtered, washed twice, adjusted to pH 8.0 and dried at 40 °C to obtain the regenerated ECCSs. Desorbed Pb and Cd concentrations in the corresponding filtrates were determines using AAS. Each experiment was carried out twice and the mean value was used in calculating metal ion recovery using Equation 4.

$$\% \, reecovery = \frac{C_{desorption}}{C_0 - C_{sorption}} \times 100 \qquad (4)$$

Where C_0 is the initial concentration, $C_{sorption}$ is the concentration after sorption and $C_{desorption}$ is the concentration after desorption.

Preparation of wastewater samples for Pb^{2+} and Cd^{2+} removal using ECCS

Samples were collected in cleaned (rinsed with conc. HNO_3, and then distilled water) PET bottles, and was quickly transferred to the laboratory. It was filtered using Whatman filter paper No 41 prior to digestion as follows; 100 cm^3 portion from each was measured into beakers, 2 mL and 1 mL of concentrated HNO_3 and HCl respectively, was added to the sample in each beaker, covered with watch glass and heated on a Bunsen burner for 160 min (to obtain a clear solution). The solution obtained for each sample was allowed to cool down to room temperature, filtered through Whatman 41 filter paper, transferred into a 100 cm^3 volumetric flask, and deionized water was added up to the mark. The pH of the solutions was adjusted to 6 using 3% NaOH, prior to some heavy metal analyses using AAS. Sorption process was carried out using 1% (w/v) ECCS, and three replicate sorption experiments were carried out on each wastewater sample.

Statistical analysis

Statistical analysis was performed using the statistical package for the social science (Version 22). Results were presented as the mean ±SD and one-way analysis of variance followed by Duncan's multiple comparison.

Result and discussion

Proximate composition and amylose content of starch extracted (Table 1) are comparable with those reviewed for legume

Table 1. Yield, proximate composition and amylose content of starch extracted

% Yield	% Carbohydrate	% Protein	% Crude fiber	% Moisture content	% Ash	% Fat	% Amylose
38	92.89±0.82	0.08±0.02	0.14±0.01	4.69± 0.31	0.11± 0.03	0.82± 0.05	36.8

Table 2. Degree of substitution of cross-linked carboxymethyl starch derivatives

% SMCA	Degree of substitution in ECCS
5	0.020
10	0.044
15	0.062
20	0.063
30	0.063

starches [23,24]. Carbohydrate and moisture content obtained indicates high starch purity (≥ 92.89%).

As shown in Table 2, the DS in ECCS increased with the amount of carboxymethylating agent up to 20%. This was due to saturation of the OH groups available for substitution reactions on the cross-linked derivative [11].

Figure 1a and b respectively presents the adsorption of Pb^{2+} and Cd^{2+} from aqueous solutions onto ECS and ECCS derivatives as well as the Na^{+} released into the aqueous solutions. More Cd^{2+} (93.94%) were adsorbed than Pb^{2+} (92.66%) on ECS, however, on carboxymethylation (ECCS-5%), there was an increase in the adsorption of both ions. Increase in the amount of the carboxymethylating agent increased the removal of Pb^{2+} (up to ECCS-15%), while that of Cd^{2+} dropped on ECCS-20% with the highest degree of substitution (DS = 0.063). Reduction in the adsorption of Cd as carboxymethyl group on starch increases can be attributed to the reduction in OH groups enhancing the adsorption of Cd^{2+} [25]. Na^{+} from residual SMCA and NaCl (carboxymethylation reaction by-product), may wash off into aqueous solution during adsorption, however, increase in Na^{+} concentration in remnant solution as adsorption increases may be attributed to ion-exchange on the carboxymethyl group ($-CH_2COONa$) [11]. As seen in Figure 1a and b, Na^{+} exchange can be said to be involved in the adsorption of Pb than Cd. At optimum adsorption (with ECCS-20%), the molar ratio of Pb^{2+} adsorbed to Na^{+} in remnant solution was calculated as; 2.62:2, instead of theoretical 1:2 expected for divalent exchange with monovalent ions. This therefore indicated involvement of other mechanisms in the adsorption of Pb. ECCS-15% was selected for further adsorption studies.

Figure 2a presents the FTIR spectra of the native starch (NS), cross-linked starch (ECS) and the carboxymethyl starch (ECCS) (15%). NS spectra show a broad peak within 3600-3200 cm^{-1}, and a peak at 2923 cm^{-1} due to O-H and C-H bonds respectively [26]. The peaks at 2195 and 1671 cm^{-1} can be associated with some minor components of starch and the hydration water molecules within the starch respectively [27]. The broad peak within 1500 and 1446 cm^{-1} can be associated with overlaps of the characteristic peak of the polysaccharides corresponding to O-H in-plane bending and methylene (H-C-H) bonds [26-28]. Another broad peak within 2250 and 998 cm^{-1} can be attributed to overlaps of C-O-C bonds joining the anhydroglucose units, C-OH, and C-C bonds [21-26].

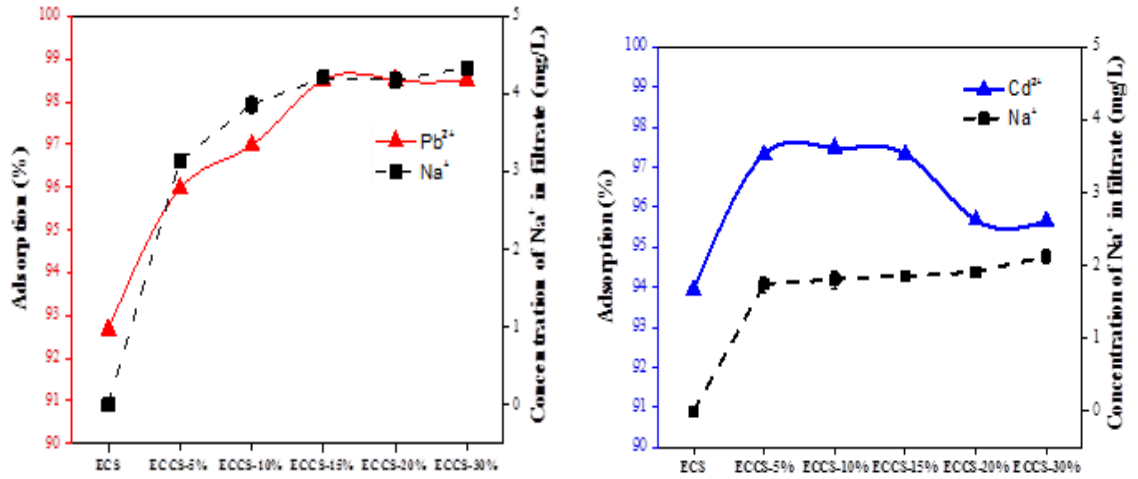

Figure 1. Adsorption of (a) Pb^{2+} and (b) Cd^{2+}, and the concentration of Na^{+} in remnant solutions

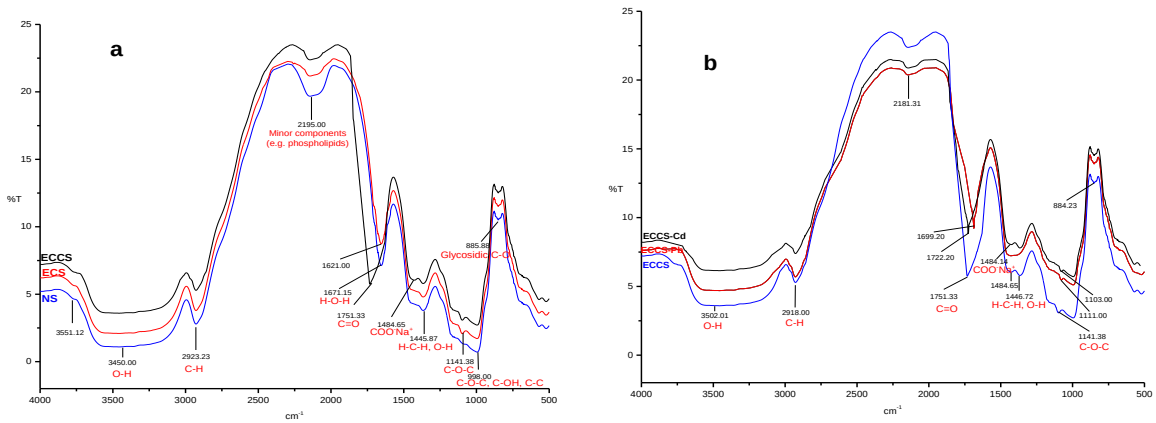

Figure 2. (a) FTIR spectra of native starch (NS), ECS and ECCS and (b) ECCS after adsorption of Pb (ECCS-Pb) and Cd (ECCS-Cd)

The peak at 886 cm^{-1} was associated with glycosidic bond characteristic of starch [27,28]. The cross-linked derivative (ECS) spectra revealed a new peak at 1141 cm^{-1}, attributed to asymmetric ether (C-O-C) bond vibration at the points of cross-links [29]. The show reduction in the O-H peak intensity and this can be attributed with the reactions of cross-linker with the OH groups on the starch molecules [30]. Also, reduction in the peaks associated with starch components and hydration water molecules can be attributed to changes in starch morphology leading to dislodgement of these molecules. The carboxymethyl derivative (ECCS) spectra show new peaks at 1751 and 1485 cm^{-1} characteristic of carbonyl (C=O) and carboxylate (COO^{-}) bonding in the sodium carboxymethyl groups ($-CH_2COONa$) introduced to the starch derivative [31]. Figure 2b compares the spectra of ECCS after adsorption of Pb (ECCS-Pb) and Cd (ECCS-Cd). After adsorption of Pb and Cd, there was reduction in the peak intensity of O-H (more significant in ECCS-Cd), and C=O, this suggested that these functional groups may be involved in adsorption of the ions. The broadening/overlap of the COO^{-} peak on ECCS-Pb spectra further agrees with the involvement of ion-exchange in the adsorption of Pb.

The SEM images of native starch, cross-linked starch (ECS), carboxymethyl starch (ECCS) and the images after adsorption of lead

(ECCS-Pb) and cadmium (ECCS-Cd) at different magnifications are presented in Figure 3a–e and a'–e'. Granules of native starch were smooth and the shapes varies (oval, spherical, round), this is typical to legume starch granules [32]. Granules of the cross-linked derivative show some rough patches, while granules of the carboxymethyl derivative showed fissures on the surfaces. Similar effect was reported by Kittipongpatana and Kittipongpatana [33]. These surface modifications can be attributed to modifications in granule morphology due to the chemical modifications. After adsorption, the granules agglomerate and the fissures on the surface was replaced by a fuse mass. This has been attributed to the electronic interactions due to the changes in the amount of the cations and anions present in the granules after adsorption, granule swelling and exudation of starch-metal complexes which are insoluble in the medium [34,35].

The EDX spectra and the elemental data of native, cross-linked, carboxymethyl starches, and the derivatives after adsorption of lead and cadmium are presented in Figure 4a–e respectively. Carbon and oxygen are typically presented in the native starch, and the presence of phosphorus can be attributed to the phosphorus components in the starch [36].

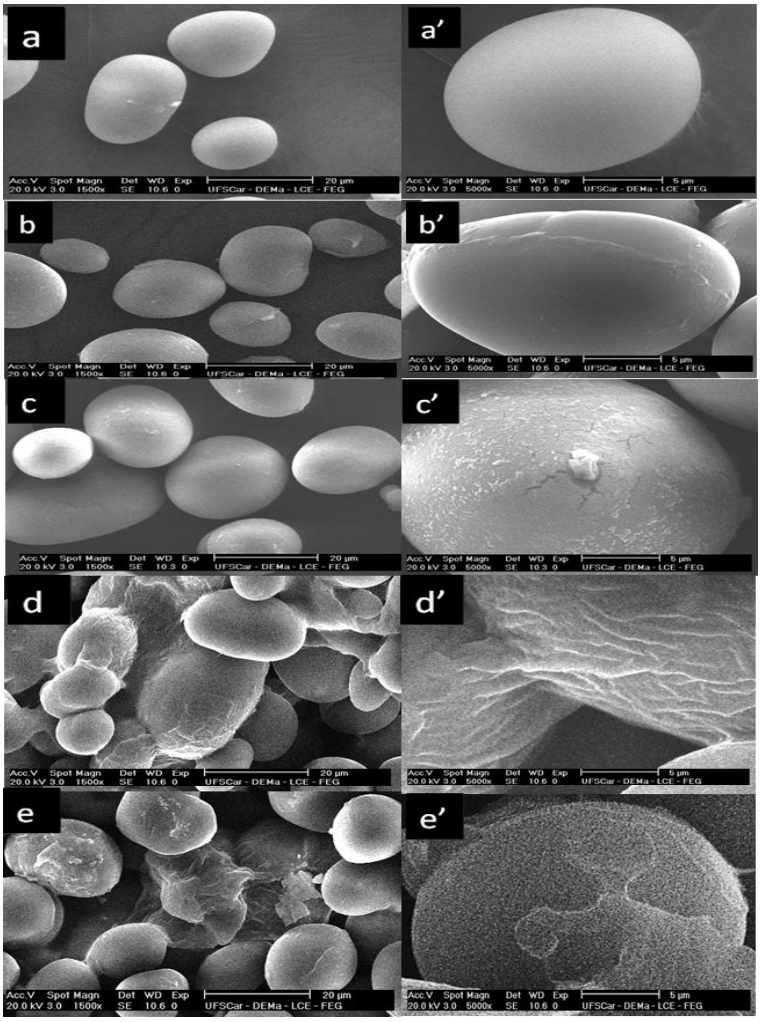

Figure 3. SEM images (a) 1500x (a') 5000x of NS, (b) 1500x (b') 5000x of ECS, (c) 1500x (c') 5000x of ECCS, (d) 1500 (d') 5000x of ECCS-Pb and (e) 1500 (e') 5000x of ECCS-Cd

The chemical composition of the epichlorohydrin cross-linked is expected to be the same as native starch, however, the presence of chlorine can be attributed to trapped HCl (not efficiently washed off), which is a by-product of the reaction. Sodium content in the carboxymethyl starch is due to the -CH_2COONa introduced, while the derivatives after adsorption show the presence of Pb and Cd.

The effect of solution pH (2–8) on the adsorption of Pb and Cd on ECCS derivative is presented in Figure 5. Precipitation of Pb and Cd was noticed above pH 6 and 7 respectively. For both ions, adsorption increased with the pH of the aqueous solutions. This was attributed to the reduction in H_3O^+ concentration in the solution as the pH increased. Reduction in H_3O^+ may reduce the competitive protonation of the adsorption sites and the electrostatic repulsion from the protonated sites, hence improving the adsorption of metal ions [37]. At the pH below 6, the hindrance effects of H^+ is higher with Cd^{2+} adsorption than Pb^{2+}, and this increased as pH drops. This can be associated with higher H^+ competition for adsorption sites with higher affinity for Cd^{2+}.

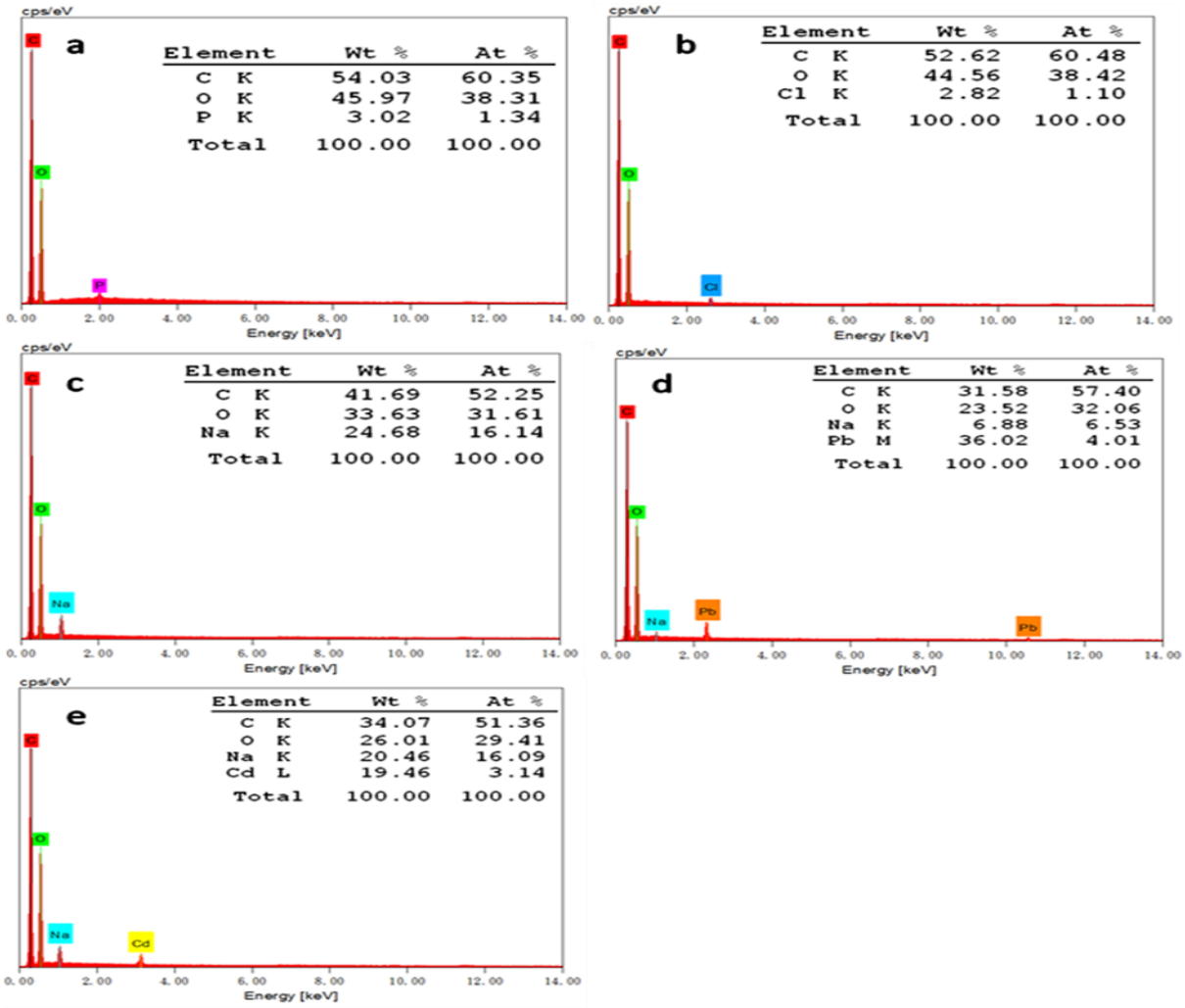

Figure 4. EDX spectra and elemental data of (a) native starch (b) ECS (c) ECCS (d) ECCS-Pb (e) ECCS-Cd

Figure 6 reveals the effect of time on the adsorption of Pb and Cd. Higher rate of adsorption was recorded for Pb than Cd up till the equilibrium time at 15 min. This can be attributed to the involvement of more processes in Pb than Cd adsorption. One or combinations of processes such as; chelation, ion-exchange, electrostatic interactions, hydrogen bonding, and entrapment of metal ions/ultrafiltration, have been reported to be involved in the adsorption of heavy metals onto starch derivatives [4,7,38]. Data from the experiment were evaluated for kinetic parameters using the linearized Lagergren's pesudo first order (Equation 5), pseudo second order (Equation 6), Elovich (Equation 7), intra-particle diffusion (Equation 8) and external diffusion model (Equation 9).

$$\ln(q_e - q_t) = lnq_e - k_1 t \quad (5)\ [37]$$

$$\frac{t}{q_t} = \frac{1}{k_2 q_e^2} + \frac{t}{q_e} \quad (6)\ [39]$$

$$q_t = \left(\frac{1}{b}\right) In(ab) + \left(\frac{1}{b}\right) In\, t \quad (7)\ [40]$$

$$q_t = k_{id} t^{1/2} + I \quad (8)\ [41]$$

$$ln\frac{1}{[1-F_{(t)}^2]} = k_{ed} t \quad (9)\ [42]$$

Where q_e and q_t (mg/g) are the amount of sorbate on sorbent at time t (min) and at equilibrium respectively, k_1 (min^{-1}), k_2 ($g/mg^{-1}/min^{-1}$), k_{id} ($mg/g^{-1}/min^{-1/2}$), and k_{ed} (min^{-1}) are rate constants for pseudo first, second, intra-particle diffusion and external diffusion models respectively. b (g/mg) is related to the extent of surface coverage and activation energy, a (mg/g min) is the initial adsorption rate, I (mg/g) estimates the layer boundary thickness, and $F_{(t)} = {}^{q_t}/_{q_e}$ is fractional attainment of equilibrium.

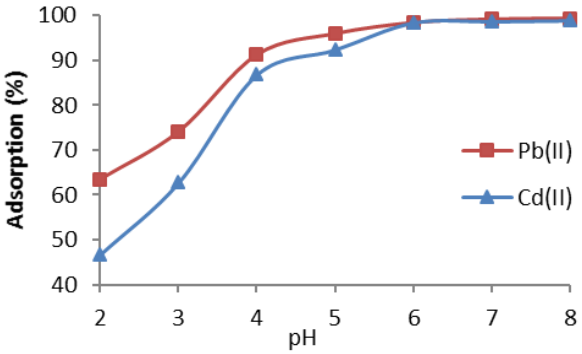

Figure 5. Effect of pH on the adsorption of Pb^{2+} and Cd^{2+} (adsorbent dosage=1% w/v, time=2 h, temperature=30 °C, C_o=50 ppm)

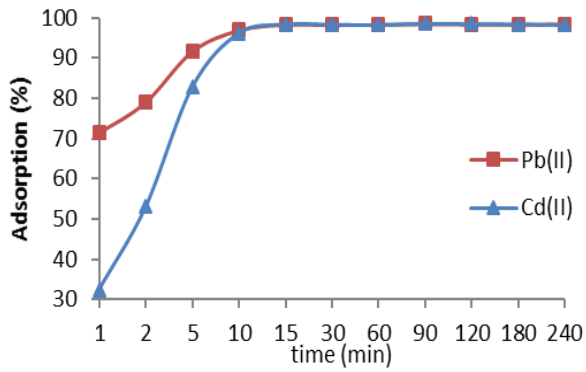

Figure 6. Effect of time on adsorption of Pb and Cd^{2+} (adsorbent dosage=1% w/v, pH=6, temperature=30 °C, C_o=50 ppm)

From a linear plot of $ln\ (q_e-q_t)$ against t (Figure S1), t/q_t against t (Figure S2), q_t against $ln\ t$ (Figure S3), q_t against $t^{½}$ (Figure S4) and $ln(1/(1-F(t)^2)$ against t (Figure S5), for pseudo-first, Pseudo-second, Elovich, intra-particle and external diffusion models respectively, some parameters in Table 3 were obtained from slopes and intercepts, while others were calculated.

$q_{e,\,exp}$ is the experimental value of the amount of metal ion adsorbed at equilibrium. Closeness of R^2 and q_e values to 1 and $q_{e,\,exp}$ respectively indicate adsorption data fitness. Table 3 showed that the adsorption data of the Cd^{2+} fits pseudo-first order better, while the adsorption data of Pb^{2+} fits pseudo-second order kinetics better. Fitness to pseudo-second order kinetics relies on the assumption that chemical interactions involving valency forces between metal ion and the adsorbent plays in the rate-determining step of the adsorption process [43]. Elovich parameters show higher values of b and a for Pb than Cd, this also signals the involvement of chemical interactions in the adsorption process of Pb^{2+} (such as ion-exchange) than Cd^{2+} [44]. R^2 values of both ions show that intra-particle diffusion play minimal role in the rate-determining step of the processes, however, higher I value indicates higher boundary layer effect in the adsorption of Pb^{2+} than Cd^{2+}. R^2 values from external diffusion models show that the rate of ion diffusion through the external surface layer of the adsorbent affects the rate of adsorption of Pb than Cd. This may attributed to the bigger size of Pb (atomic radius = 1.75 Å) compared to Cd (atomic radius = 1.71 Å).

Effect of the initial concentrations on the adsorption of Pb and Cd is presented in Figure 7. For both ions, adsorption capacity started dropping at initial aqueous solution concentrations above 50 ppm, however, adsorption of Pb^{2+} stayed higher than Cd^{2+}, and this can be attributed to the availability of more adsorption sites for Pb^{2+} than Cd^{2+}. Reduction in adsorption can be associated to the increasing rate of saturation of adsorption sites on ECCS derivative as initial concentration of ions increased above 50 ppm. Reduction in adsorption can also be attributed to increase in repulsive forces as the amount of ions adsorbed increases on the surface of the adsorbent.

Table 3. Kinetic parameters of Pb^{2+} and Cd^{2+} adsorption on ECCS

Parameters	Pb^{2+}	Cd^{2+}
$q_{e,exp}$ (mg g^{-1})	4.9200	4.9300
Pseudo-first Order		
q_e (mg g^{-1})	1.7911	4.8293
k_1 (min^{-1})	0.3143	0.3681
R^2	0.9981	0.9998
Pseudo-second Order		
$q_{e,cal}$ (mg g^{-1})	5.0839	5.7747
k_2 (g $mg^{-1}min^{-1}$)	0.3861	0.0755
R^2	0.9999	0.9975
Elovich		
A_E (g mg^{-1})	2.3441	0.9602
B_E (mg $g^{-1}min^{-1}$)	11.2615	2.6807
R^2	0.9117	0.9057
Intra-particle diffusion		
k_{id} (mg $g^{-1}min^{-1/2}$)	0.3590	0.8780
I	2.9360	0.1180
R^2	0.9313	0.9240
External diffusion		
K_{ed} (min^{-1})	0.2998	0.3275
R^2	0.9990	0.9953

Data from the experiment were evaluated for isotherm parameters using the linearized Langmuir (Equation 10), Freundlich (Equation 11), and Halsey (Equation 12) adsorption isotherm models.

$$\frac{C_e}{q_e} = \frac{1}{q_m k_L} + \frac{C_e}{q_m} \quad (10)\ [45]$$

$$log q_e = log k_F + \frac{1}{n} log C_e \quad (11)\ [45]$$

$$In\ q_e = \frac{1}{n_H}\ In\ K_H - \frac{1}{n_H}\ In\ C_e \quad (12)\ [45]$$

q_e (mg/g), q_m (mg/g) and C_e (mg/L) are amount of ion adsorbed at equilibrium, maximum amount of ion adsorbed and concentration of ion in aqueous solution at equilibrium respectively. K_L is the langmiur constant. K_L and C_o can be used in determining the feasibility of a reaction from the value of a dimensionless parameter called separation factor (R_L) (Equation 15).

$$R_L = \frac{1}{1+K_L C_0} \quad (13)$$

K_F, is Freundlich constant, $1/n$ defines adsorption intensity, relative distribution of energy and the heterogeneity of the adsorption sites, while n value between 1 and 10 indicates a favorable process. K_H and n_H are Halsey isotherm constants. Plots of C_e/q_e against C_e (Figure S6a and b), *log* q_e against *log* C_e (Figure S7a and b), and *ln* q_e against *ln* C_e (Figure S8a and b) for Langmuir (Equation 10), Freundlich (Equation 11), and Halsey isotherm models presented linear curves. Some parameters in Table 4 were obtained from the slope and intercept of the curves while others were calculated.

Correlation coefficient (R^2) values (Table 4), revealed that the Pb adsorption data fits Langmuir model better, while Cd data fits Freundlich and Halsey models. Langmuir model relies on a mono-layer adsorption in which adsorption and desorption are balanced to achieve a dynamic equilibrium on a homogenous surface [45]. This stoichiometric interaction therefore assumes chemisorption. R_L values calculated for both Pb and Cd falls within the range $0<R_L<1$, indicating favourable adsorption processes. Freundlich and Halsey models assume multi-layer adsorption process on a heterogeneous surface [45]. This is attributed to physisorption processes.

The effect of temperature on the adsorption of Pb and Cd is depicted in Figure 8. Adsorption capacity reduced as the temperature of the aqueous solutions increases. This can be attributed to gradual loss in the structural integrity of the starch derivative due to elution of (hydrophilic) contents at the onset of gelatinization. Increase in temperature will also hinder exothermic processes involved in the adsorption of the heavy metal ions.

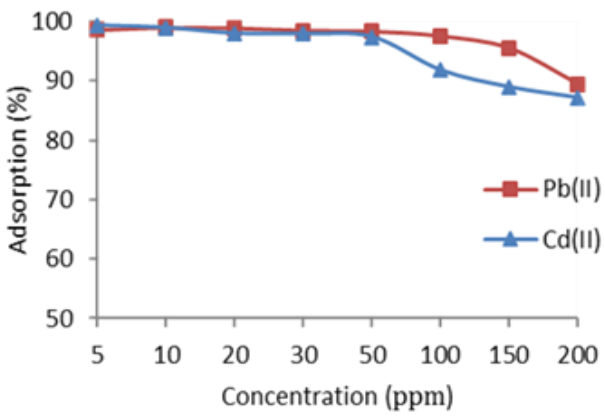

Figure 7. Effect of initial concentration on adsorption of Pb^{2+} and Cd^{2+} (adsorbent dosage = 1% w/v, time = 15 min, pH = 6, temperature = 30 °C)

Table 4. Isotherm parameters of Pb^{2+} and Cd^{2+} adsorption on ECCS

Isotherm model parameters	Pb^{2+}	Cd^{2+}
$q_{m,\,exp}$ (mg/g)	17.8900	17.4300
Langmuir		
q_m (mg/g)	19.4175	17.7620
k_L (L/mg)	0.4361	0.2938
R^2	0.9983	0.9309
R_L (C_o ppm)		
R_l (5)	0.3144	0.4050
R_l (10)	0.1865	0.2539
R_l (30)	0.0710	0.1019
R_l (50)	0.0439	0.0637
R_l (100)	0.0224	0.0329
R_l (150)	0.0151	0.0222
R_l (200)	0.0113	0.0167
Freundlich		
k_F $(L/mg)^{1/n}$	4.2150	3.3251
1/n	0.0611	0.5217
n	16.3479	1.9168
R^2	0.9405	0.9909
Halsey		
k_H	7.7818	5.5799
n_H	-1.6410	-1.9176
R^2	0.9421	0.9978

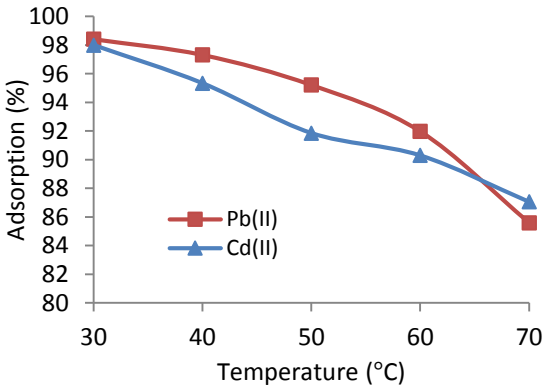

Figure 8. Effect of temperature on adsorption of Pb^{2+} and Cd^{2+} (adsorbent dosage = 1% w/v, time = 15 min, pH = 6, C_o = 50 ppm)

The thermodynamic parameters for the effects of temperature on the adsorption of Pb and Cd were analyzed using the van't Hoff's equation (Equation 14) [46].

$$\log k_c = \frac{\Delta S}{2.303R} - \frac{\Delta H}{2.303RT} \qquad (14)$$

k_c is the equilibrium constant (q_e/C_e), R is the gas constant (8.314 $J/mol^{-1}/K^{-1}$), T (K) is the temperature while ΔH and ΔS are the enthalpy and entropy change respectively calculated from the slope and intercept of linear plot; log k_c against 1/T. Free energy (ΔG) was calculated from the thermodynamic equation (Equation 15).

$$\Delta G = \Delta H - T\Delta S \quad (15)$$

As seen in Table 5, ΔH is negative for both ions, implying that the adsorption of both ions is driven by an exothermic process. The magnitude of ΔH for Pb adsorption is higher than that of Cd (indicating stronger bonding between Pb^{2+} and ECCS derivative), and falling within the range corresponding to chemisorption processes, as it is slightly higher than the lower limit (-40 kJ/mol^{-1}) [47]. Positive values of ΔG showed that adsorption is no more spontaneous for Pb at 343 K, and Cd at 333 K. Negative values of ΔS can be explained as the movement of ions from their random state in the aqueous solution to a more orderly state on the surface of the adsorbent. Higher values of ΔS for Pb indicates an enhanced orderliness (on homogenous sites), which can be attributed to specific interactions typical to chemical adsorption processes.

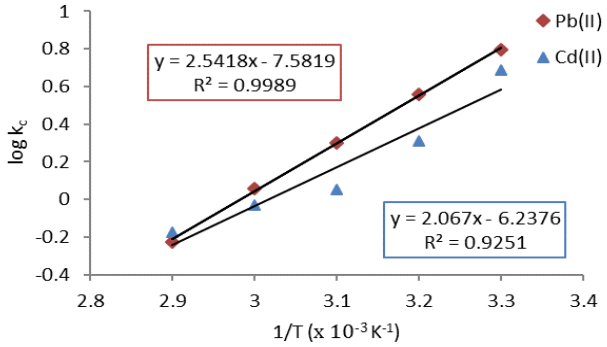

Figure 9. Plot of log (k_c) against 1/T for adsorption of Pb^{2+} and Cd^{2+}

Table 5. Thermodynamic parameters of Pb^{2+} and Cd^{2+} adsorption on ECCS

Metal ions	T (K)	ΔG (kJ/mol^{-1})	ΔH (kJ/mol^{-1})	ΔS (J/mol^{-1}/K^{-1})
Pb^{2+}	303	-4.68	-48.67	-145.17
	313	-3.23	-48.67	-145.17
	323	-1.78	-48.67	-145.17
	333	-0.33	-48.67	-145.17
	343	1.12	-48.67	-145.17
Cd^{2+}	303	-3.39	-39.58	-119.43
	313	-2.20	-39.58	-119.43
	323	-1.00	-39.58	-119.43
	333	0.19	-39.58	-119.43
	343	1.39	-39.58	-119.43

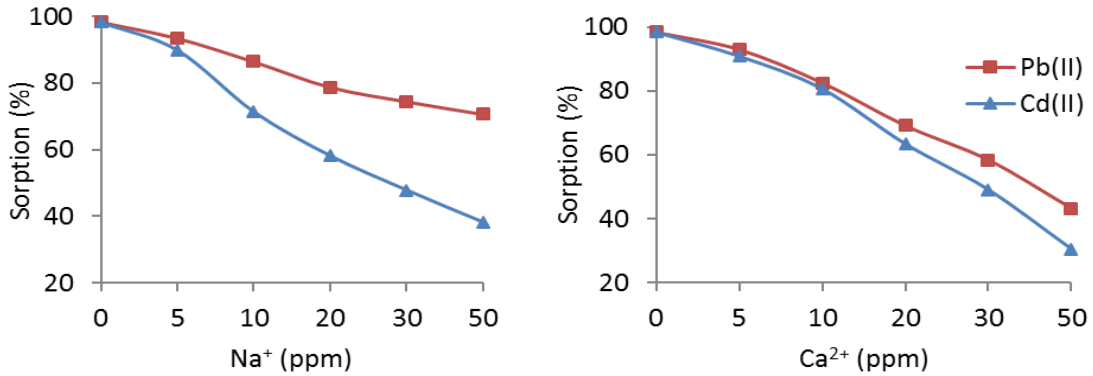

Figure 10. Effect of interfering ions (Na^+ and Ca^{2+}) on adsorption of Pb^{2+} and Cd^{2+} (adsorbent dosage = 1% w/v, temperature = 30 ºC, time = 15 min, pH = 6, C_o = 50 ppm)

Figure 10 presents the effects of different concentrations of Na^+ and Ca^{2+} as interference in the adsorption of Pb^{2+} and Cd^{2+}. Results show that the adsorption of both heavy metal ions were reduced as the concentrations of monovalent (alkali metal) and divalent (alkali-earth metal) increased in the aqueous solutions due to general competition for adsorption sites on the surface of the adsorbent. The adsorption of Pb reduced more rapidly in aqueous solutions containing Ca^{2+} than observed in solutions containing Na^+, this may be due to competition of Ca^{2+} for adsorption sites that are selects for Pb^{2+}.

Increase in the amount of ECCS derivative in aqueous solution corresponds to increase in adsorption sites, which will consequently increase the amount of heavy metal ion adsorbed, as shown in Figure 11. Optimum and approximately 100% removal of both ions was recorded when ECCS derivative was increased to amount corresponding to 1.5% (w/v) of the aqueous solution.

ECCS derivatives loaded with heavy metal ions after adsorption was subjected to desorption, to regenerate a free ECCS derivative. The amount of heavy metal ion released during desorption at different time is presented in Table 6. Results showed that Pb (99.6%) and Cd (99.9%) ions can be efficiently recovered from the ECCS. Equilibrium desorption of Cd was achieved after 5 min, while that of Pb was only achieved after 15 min. This again signals the presence of stronger (chemical) bonding between Pb and ECCS.

Cycles of reuse of the regenerated ECCS derivative is presented in Figure 12. Adsorption of Pb^{2+} on ECCS reduced from 98.3 to 88.78% while Cd^{2+} reduced from 98.32 to 75.57% after 5 cycles of reuse. Reduction in adsorption capacity of the starch derivative over recuse has been attributed to gradual loss in structural integrity due to partial hydrolysis, dissolution and elution of granular components (such as amylose content) [11,16].

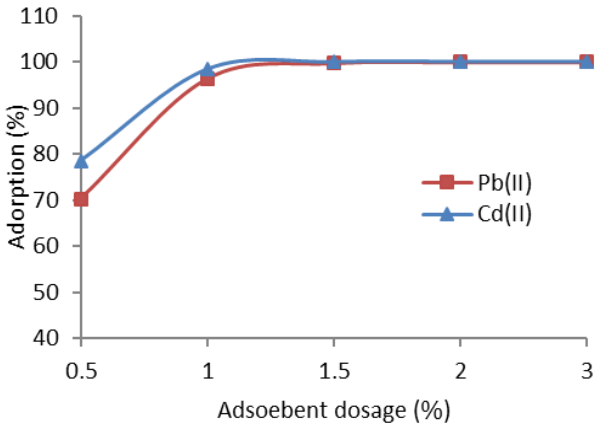

Figure 11. Effect of ECCS dosage on adsorption of Pb^{2+} and Cd^{2+} (time = 15 min, pH = 6, temperature = 30 °C, C_o = 50 ppm)

Table 6. Desorption of ions using 1M HNO_3 (adsorption conditions: C_0 = 50 ppm, pH = 6, temperature = 30 °C, contact time = 15 mins, adsorbent dosage = 1%; amount adsorbed = 49.15 ppm for Pb^{2+} and 49.16 ppm for Cd^{2+}

Desorption time (mins)	Pb^{2+}		Cd^{2+}	
	C_t (ppm)	Recovery (%)	C_t (ppm)	Recovery (%)
2	8.68±0.08	17.66	28.66±0.20	58.3
5	17.87±0.22	36.36	49.12±0.23	99.92
10	38.67±0.09	78.68	49.11±0.14	99.9
15	48.96±0.10	99.6	49.12±0.12	99.92

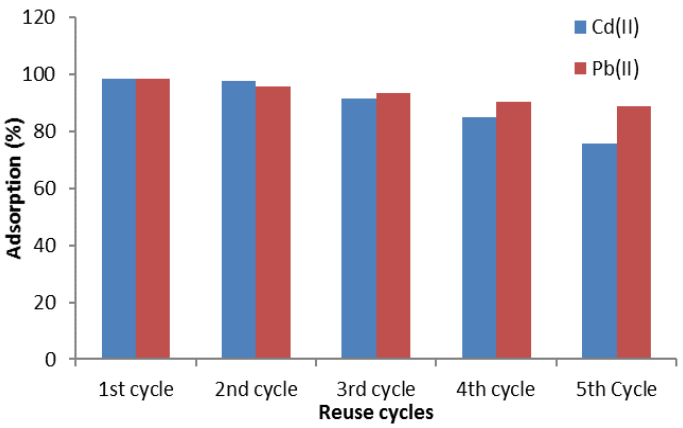

Figure 12. Cycles of regeneration and reuse of ECCS in adsorption of Pb^{2+} and Cd^{2+}

Table 7. Removal of heavy metals from wastewater using ECCS derivative (adsorption time = 15 min, at room temperature = 30 ± 2 ºC)

	Sample A (ppm)		Sample B (ppm)		Standards (EGASPIN, 2002)
Elements	C_0	C_t	C_0	C_t	(ppm)
Pb	1.8218	ND	0.9293	ND	0.05
Cd	0.6246	ND	0.4967	ND	0.00
Cr (total)	0.4367	ND	0.6218	ND	0.3000
Zn	0.0315	ND	0.8050	ND	1.000
Cu	0.0561	ND	2.0693	ND	1.500
Fe	2.4534	ND	3.3956	ND	1.000

Key: Sample A = wastewater from gold processing site; Sample B = wastewater from crude oil exploration; C_0 = initial concentration; C_t = final concentration; ND = Not Detected (absent or lower than the limit of detection; for Pb = 0.04 ppm, Cd = 0.02, Cr = 0.04, Zn = 0.02, Cu = 0.02 and Fe = 0.03)

Table 7 present the results obtained when ECCS derivative was practically used in the removal of heavy metal ions in some samples of wastewater. Results show that the concentrations of all the heavy metal ions analyzed reduce beyond the detection limits of the instrument used. Compared to standards, it can be said that the concentrations of the heavy metal ions has been reduced to acceptable levels. The ECCS derivative in this study therefore shows good potentials as an efficient adsorbent in the removal of heavy metal contaminants, even at low concentrations in wastewater.

Conclusion

Cross-linking with epichlorohydrin and carboxymethylating starch extracted from Kwakil bean produced ECCS, which is a derivative with adsorption potentials. However, the processes involved in the adsorption of heavy metal ions may differ. Sodium ion-exchange on carboxymethyl group is suspected to be involved in the adsorption of lead; however this cannot be established for cadmium. Optimum adsorption capacity (>90%) was achieve at pH 6, time 15 min, initial concentration 50 ppm, at 30 ºC, ECCS dosage 1%, and in the presence of minimal concentrations of alkali and alkali-earth metals. Kinetic, isotherm and thermodynamic parameters showed that chemical interactions (chemisorption) mechanisms are involved more in the adsorption of lead than cadmium. ECCS can be efficiently regenerated and reused, and after 5 reuse cycles more than 70% removal

of heavy metals was still recorded. Practical application of ECCS in the removal of heavy metals from wastewater with low concentrations of heavy metal ions, indicating that the derivative have a great capability as aqueous heavy metal adsorbent.

Acknowledgement

Authors acknowledge the technical crew of the Physical/Inorganic Chemistry Laboratory, Federal University of Technology Akure, Nigeria, Petroleum Chemistry Laboratory, American University of Nigeria, Chemistry Laboratory, Afe Babalola University, Nigeria and Departmento de Engenharia de Materials, Universidade Federal de Sao Carlos, Brazil.

Disclosure statement

Authors declare no conflict of interests.

ORCID

Ayodele Akinterinwa **:** 0000-0001-5236-9238

References

[1] Orisakwe O.E. *North Am. J. Med. Sci.,* **2014**, *6*, 61–70.
[2] C. Pan, J., Chen, K. Wu, Z. Zhou, T. Cheng, *IOP Conf. Ser. Mater. Sci. Eng.,* **2018**, *301*, 1–8.
[3] D. Yu, S. Morisada, H. Kawakita, K. Ohto, K. Inoue, X. Song, G. Zhang, *Processes*, **2019**, *7*, 2–15.
[4] B. Xiang, W. Fan, X. Yi, Z. Wang, F. Gao, Y. Li, H. Gu, *Carbohyd. Polym.,* **2016**, *136*, 30–37.
[5] A.H. Shalla, Z. Yaseen, M.A. Bhat, T.A. Rangreez, M. Maswal*, Sep. Sci. Technol.,* **2019**, *54*, 89–100.
[6] Zia-ud-Din, H. Xiong, P. Fei, *Crit. Rev. Food Sci. Nutrit.,* **2017**, *57*, 2691–2705.
[7] T. Wang, Y. Song, B. Li, X. Zhou, *Water Air Soil Pollut.,* **2012**, *223*, 679–686.
[8] Huber, K.C. and BeMiller, J.N. CRC Press, Boca Raton, FL, **2010**, 145–203.
[9] S.H. Koo, K.Y. Lee, H.G. Lee, *Food Hydrocoll.,* **2010**, *24*, 619–625.
[10] A. Akinterinwa, S.A. Osemeahon, A.F. Akinsola, U. Reuben, *J. Agricul. Food Technol.,* **2014**, *4*, 13–20.
[11] B.S. Kim, S.T. Lim, *Carbohyd. Polym.,* **1999**, *39*, 217–223.
[12] X. Gao, D.W. Metge, C. Ray, R.W. Harvey, J. Chorover, *Environ. Sci. Technol.,* **2009**, *43*, 7423–7429.
[13] A. Adewuyi, F.V. Pereira, *J. Adv. Res.,* **2016**, *7*, 947–959.
[14] M. Haroon, L. Wang, H. Yu, N.M. Abbasi, M. Saleem, R.U. Khan, R.S. Ullah, Q. Chen, J. Wu, *Rsc Adv.,* **2016**, *6*, 78264–78285.
[15] M.W. Sabaa, E.H.A. Magid, R.R. Mohamed, *Res. Rev. J. Chem.*, **2017**, 6, 47–59.
[16] S. Wang, L. Copeland, *Crit. Rev. Food Sci. Nutr.,* **2015**, *55*, 1081–1097.
[17] S.C. Alcázar-Alay, M.A.A. Meireles, *Food Sci. Technol.,* **2015**, *35*, 215–236.
[18] S. Kumar, A.K. Verma, M. Das, S. Jain, P.D. Dwivedi, *Nutrition*, **2013**, *29*, 821–827.
[19] T.J. Schoch, E.C. Maywald, *Cereal Chem.,* **1968**, *45*, 564–573.
[20] W. Horwitz, G. Latimer, AOAC official methods. *Official Methods of Analysis" of AOAC International, 17th Ed. AOAC International, Gaithersburg, MD, USA*, **2000**.
[21] F.J. Warren, M.J. Gidley, B.M. Flanagan, *Carbohyd. Polym.,* **2016**, *139*, 35–42.
[22] Z. Stojanović, K. Jeremić, S. Jovanović, M.D. Lechner, *Starch-Stärke,* **2005**, *57*, 79–83.
[23] R. Hoover, F. Sosulski, *Starch-Stärke,* **1986**, *38*, 149–155.
[24] I.A. Wani, D.S. Sogi, A.A. Wani, B.S. Gill, U.S. Shivhare, *Int. J. Food Sci. Technol.,* **2010**, *45*, 2176–2185.
[25] V. Singh, S.K. Singh, *Adv. Mater. Lett.,* **2015**, *6*, 607–615.
[26] J. Coates, Encyclopedia of analytical chemistry. *Interpretation of infrared spectra, a practical approach,* John Wiley & Sons Ltd, Chichester, **2000**, pp 10815–10837.
[27] L. González-Cruz, J.L. Montañez-Soto, E. Conde-Barajas, M.D.L.L.X. Negrete, A.

Flores-Morales, A. Bernardino-Nicanor, *Int. J. Boil. Macromolecule,* **2018**, *107*, 965–972.
[28] A. Bernardino-Nicanor, G. Acosta-García, N. Güemes-Vera, J.L. Montañez-Soto, M. de los Ángeles Vivar-Vera, L. González-Cruz, *J. Food Sci. Technol.,* **2017**, *54*, 933–943.
[29] D. Li, P. Lv, L. Fan, Y. Huang, F. Yang, X. Mei, D. Wu, *Biomater. Sci.,* **2017**, *5*, 2337–2346.
[30] E. Basiak, A. Lenart, F. Debeaufort, *Polymers*, **2018**, *10*, 412.
[31] N. Ochoa, M. Bello, J. Sancristóbal, V. Balsamo, A. Albornoz, J.L. Brito, Materials Research, **2013**, *16*, 1209–1219.
[32] J.P. Wojeicchowski, G.L.D.A.D. Siqueira, L.G. Lacerda, E. Schnitzler, I.M. Demiate, *Food Sci. Technol.,* **2018**, *38*, 318–327.
[33] N. Kittipongpatana, O.S. Kittipongpatana, *Int. J. Pharm. Pharm. Sci.,* **2015**, *7*, 404–407.
[34] W. Ciesielski, C.Y. Lii, M.T. Yen, P. Tomasik, *Carbohyd. Polym.,* **2003**, *51*, 47–56.
[35] Q. Chen, X. Zheng, L. Zhou, M. Kang, *BioResources,* **2019**, *14*, 302–312.
[36] T. Kasemsuwan, J.L. Jane, *Cereal chem.,* **1996**, *73*, 702–707.
[37] S. Madala, S.K. Nadavala, S. Vudagandla, V.M. Boddu, K. Abburi, *Arab. J. Chem*., **2017**, *10*, S1883–S1893.
[38] L. Guo, S.F. Zhang, B.Z. Ju, J.Z. Yang, X. Quan, *J. Polym. Res.,* **2006**, *13*, 213–217.
[39] Y.S. Ho, G. McKay, *Process biochem.,* **1999**, *34*, 451–465.
[40] H. Lin, J. Xu, Y. Dong, L. Wang, W. Xu, Y. Zhou, *Desalinat. Water Treat.,* **2016**, *57*, 18537–18550.
[41] W.J. Weber, J.C. Morris, *J. Sanit. Eng. Divis.,* **1963**, *89*, 31–60.
[42] Y.S. Al-Degs, M.I. El-Barghouthi, A.A. Issa, M.A. Khraisheh, G.M. Walker, *Water Res.,* **2006**, *40*, 2645–2658.
[43] M. Arshadi, M. Amiri, S. Mousavi, *Water Resour. Indust.,* **2014**, *6*, 1–17.
[44] M. Alkan, O. Domirbas, M. Dogan, *Micropor. Mesopor. Mater.,* **2007**, *101*, 388–396.
[45] N. Ayawei, A.N. Ebelegi, D. Wankasi, *J. Chem.*, **2017**, *17*, 3039817.
[46] P.S. Kumar, K. Ramakrishnan, S.D. Kirupha, S. Sivanesan, *Brazil. J. Chem. Eng.,* **2010**, *27*, 347–355.
[47] P. Atkins, *Physical Chemistry*, 6th Ed., Oxford University press: London, **1999**, pp 857–886.

How to cite this manuscript: Ayodele Akinterinwa, Ebun Oladele, Albert Adebayo, Olubode Ajayi, Synthesis of Cross-Linked Carboxymethyl Legume Starch for Adsorption of Selected Heavy Metals from Aqueous Solutions*, Adv. J. Chem. A*, **2020**, *3*, S594–S611.